Modelling the influence of total suspended solids on *E. coli* removal in river water

Jueying Qian, Evelyn Walters, Peter Rutschmann, Michael Wagner and Harald Horn

ABSTRACT

Following sewer overflows, fecal indicator bacteria enter surface waters and may experience different lysis or growth processes. A 1D mathematical model was developed to predict total suspended solids (TSS) and *Escherichia coli* concentrations based on field measurements in a large-scale flume system simulating a combined sewer overflow. The removal mechanisms of natural inactivation, UV inactivation, and sedimentation were modelled. For the sedimentation process, one, two or three particle size classes were incorporated separately into the model. Moreover, the UV sensitivity coefficient α and natural inactivation coefficient k_d were both formulated as functions of TSS concentration. It was observed that the *E. coli* removal was predicted more accurately by incorporating two particle size classes. However, addition of a third particle size class only improved the model slightly. When α and k_d were allowed to vary with the TSS concentration, the model was able to predict *E. coli* fate and transport at different TSS concentrations accurately and flexibly. A sensitivity analysis revealed that the mechanisms of UV and natural inactivation were more influential at low TSS concentrations, whereas the sedimentation process became more important at elevated TSS concentrations.

Key words | *E. coli*, modelling, particle size distribution, removal mechanism

Jueying Qian (corresponding author)
Michael Wagner
Harald Horn
Karlsruhe Institute of Technology, Engler-Bunte-Institut, Chair of Water Chemistry and Water Technology,
Engler-Bunte-Ring 9, 76131 Karlsruhe,
Germany
E-mail: *jueying.qian@partner.kit.edu*

Evelyn Walters
Technische Universität München, Chair of Urban Water Systems Engineering,
Am Coulombwall, 85748 Garching,
Germany
and
Temple University, College of Engineering, Civil and Environmental Engineering,
Philadelphia, PA 19122,
USA

Peter Rutschmann
Technische Universität München, Chair of Hydraulic and Water Resources Engineering,
Arcisstr. 21, 80333 München,
Germany

Michael Wagner
Karlsruhe Institute of Technology, Institute of Functional Interfaces,
Hermann-von-Helmholtz-Platz 1,
76344 Eggenstein-Leopoldshafen,
Germany

INTRODUCTION

Surface water quality is closely related to the quality of life in a city. In Europe, the bathing water quality is usually satisfactory according to the EU bathing water directive (EEA 2015). However, after periods of intense rain the water quality is expected to be non-compliant due to microbiological contamination. This is because heavy rain events are often associated with municipal sewer overflows, bacteria resuspension, and surface run-off (Davies & Bavor 2000; Nagels *et al.* 2002; Garzio-Hadzick *et al.* 2010). It is thus important to determine how fast the waters achieve sufficient quality again. Fecal indicator bacteria (FIB) such as fecal coliforms (FC), *Escherichia coli* (*E. coli*), and *Enterococcus* are accepted indicators of microbiological contamination and can be used to evaluate the microbial water quality after rainfall.

After entering surface waters, FIB may experience growth, lysis, predation, and UV inactivation. Researchers studied the survival rate of FIB in different physical and chemical conditions, e.g. sunlight, pH value, temperature, turbidity, salinity, hydraulic parameters, and nutrient concentrations, to evaluate their continued risks to human health (Evison 1989; Pommepuy *et al.* 1992; Canteras *et al.* 1995; Howell *et al.* 1996; Sinton *et al.* 2002; Kay *et al.* 2005; Schultz-Fademrecht *et al.* 2008; Garzio-Hadzick *et al.* 2010; Walters *et al.* 2014a). FIB may also attach to particles, or remain freely suspended in the water body (Characklis *et al.* 2005). Particle-associated bacteria may settle out of the bulk liquid and thus render sedimentation a considerable removal mechanism.

In an FIB fate and transport model, the particle-associated bacteria are commonly assumed to have the same settling velocity as the particles they are associated with. Traditionally and for the reason of simplification, one

doi: 10.2166/wst.2015.605

median particle size is often chosen and incorporated in models to simulate the sedimentation process (Steets & Holden 2003; Cho *et al.* 2012; Ghimire & Deng 2013). However, the particle size of sediment varies over two to three orders of magnitude and the settling velocity varies over four to six orders of magnitude (Ghimire & Deng 2013). So far, little attention has been paid to the influence of the particle size distribution in FIB removal models. Therefore, it is likely that the precision of water quality models can be further improved by incorporating different particle size classes into them.

Suspended solids do not only influence the settling characteristics of bacteria. It is reported that the existence of suspended solids/particles increases the survival of coliforms in bulk liquid (Qualls *et al.* 1985). Moreover, compared to freely suspended bacteria, particle-associated bacteria are known to have higher survival rates. Possible reasons are (i) particles shield the bacteria from UV irradiation, (ii) the pores of the particles protect the FIB from predation (Wright *et al.* 1995; Decamp & Warren 2000), (iii) the particles offer a better micro-environment with availability of nutrients and substrates, and (iv) certain sediments (i.e. smectite clays) enhance the formation of protective biofilms (Jamieson *et al.* 2005; Alimova *et al.* 2007).

As far as we are aware, a study relating bacteria removal from the water column with particle (total suspended solids) concentrations as well as particle size distribution has to date not been reported. In this study, an *E. coli* fate and transport model was developed and calibrated using experimental data from a large-scale experimental setup (Walters *et al.* 2014b). The primary objectives of this study were (i) to study the impact of the particle size distribution on the removal of FIB, (ii) to assess the impact of sedimentation, UV and natural inactivation as removal mechanisms, and (iii) to study the relationship between total suspended solids (TSS) concentration and FIB removal from the water column.

MATERIALS AND METHODS

Large-scale flume setup

A detailed description of the experimental setup has been published in Walters *et al.* (2014b). Briefly, the flume was built of concrete (length = 12 m, width = 0.5 m, water depth h = 0.5 m, $V \approx 14\ m^3$) and was operated either in flow-through or recirculation mode. In recirculation mode, four pumps transported water from the collection basin back to the inlet basin.

The water used in the experiments was from the Obernach River (Bavaria, Germany; side stream of the Isar River). The oligotrophic Obernach water was directed to a reservoir to allow large particles to settle. Gravels taken from the Isar River (d_{50} = 15–30 mm) were spread in the flume bed to mimic a natural river environment. Before each experiment the flume was operated in flow-through mode for a minimum of 3 weeks to allow fine particles to settle.

Experiment A

This experiment was performed in order to investigate FIB removal from the water column of an oligotrophic river following a combined sewer overflow (CSO). The CSO was simulated by addition of raw wastewater ($V = 1\ m^3$) from the municipal wastewater treatment plant in Garching (Bavaria, Germany) to the flume operated in recirculation mode. The ratio of wastewater and river water was 1:13 (V:V) and the volumetric flow rate was constant at $0.2\ m^3\ s^{-1}$; experimental duration was 70 hours. This experiment is referred to as Experiment 2 in the original publication of Walters *et al.* (2014b).

Experiment B

To investigate the impact of resuspended sediment on the FIB removal rate, the flume was initially operated at a volumetric flow rate of $0.1\ m^3\ s^{-1}$ with $1\ m^3$ of wastewater added to $13\ m^3$ of river water as in Experiment A. After 140 min the volumetric flow rate was doubled to induce resuspension of settled particles. The experiment duration was 70 hours. This experiment is referred to as Experiment 3 in the original publication of Walters *et al.* (2014b).

Sampling procedure of Experiments A and B

Uniform sampling for *E. coli* enumeration and TSS measurement always occurred in the middle of the flume (length of 6 m) at predefined time interval by a team of researchers (for details see Walters *et al.* (2014b)). Samples were stored at 4 °C and analysed within 24 hours. Viable *E. coli* were enumerated using the standardized microplate methods for surface water, DIN EN ISO 9308–3 (Bio-Rad, Munich, Germany), based on the presence of the beta-glucuronidase enzyme. The average surface UV irradiance in daytime in Experiments A and B was $6.5\ W\ m^{-2}$ and $17\ W\ m^{-2}$, respectively; the average water temperature in Experiments

A and B was 15.7 and 19.7 °C. Parameters used within the simulations are summarized in Table 1.

In addition to the coarse gravel, fine sediments were also present on the flume bed. These fine sediments were a mixture of particles originating from the river (water) and raw wastewater. The particle size distribution of the fine sediments was measured after the experiments by sieving and filtering techniques (Walters 2013). The Obernach River is an oligotrophic river and has very low concentrations of *E. coli*. Background *E. coli* concentrations ranged between 0.26 and 5.87 most probable number (MPN) ml^{-1}. Most of the *E. coli* in the experiment thus originated from the added raw wastewater. The partitioning behaviour of *E. coli* to different particle sizes in wastewater was characterized by Walters *et al.* (2013) and are listed in Table 2. Jeng *et al.* (2005) found comparable *E. coli* partitioning characteristics in urban storm water run-off. Therefore, it was assumed that the association of *E. coli* to different particle size classes in the flume was identical to that of *E. coli* to wastewater particles measured by Walters *et al.* (2013).

Modelling process

A model was developed to describe the fate and transport of solid particles/TSS and *E. coli* in a flume mimicking an oligotrophic river following a CSO. Model setup, parameter estimations (chi-squared test), and a sensitivity analysis (absolute-relative sensitivity function) were performed using AQUASIM (version 2.1d, Reichert (1994)). The model is 1D in the vertical direction and considers dispersion as well as reactions. The Reynolds number in the flume was $>5\times10^5$ and the dispersion coefficient was calculated to be 180 $m^2\ h^{-1}$ (Jobson & Sayre 1970) when the volumetric flow rate reached 0.2 $m^3\ s^{-1}$. Flow was therefore regarded as being turbulent and the system was thus treated as a continuous stirred-tank reactor. For simplicity reasons, concentration gradients in the longitudinal direction as well as the influence of the lateral velocity were neglected. This has further been proved by additional simulations (data not shown).

Table 1 | Parameters used in the 1D model

Symbol	Unit	Value/expression	Variable/parameters	Reference
C^0_{EC}	MPN m^{-3}	Experiment A: 7.3×10^8 Experiment B: 6.4×10^8	total initial *E. coli* concentration	Walters *et al.* (2014b)
C^0_{TSS}	kg m^{-3}	Experiment A: 0.015 Experiment B: 0.060	total initial TSS concentration	Walters *et al.* (2014b)
d_j	μm	see Table 2	median diameter of particle class *j*	Walters (2013)
D	$m^2\ h^{-1}$	180	dispersion coefficient	Jobson & Sayre (1970)
F_{sun}	–	$F_{sun}=1$, during daytime, $F_{sun}=0$, during nighttime	Boolean variable. It activates or inactivates the mechanism of UV inactivation	measured
$f_{P,j}$	–	see Table 2	*E. coli* fraction to particle size class *j*	Walters *et al.* (2013)
$f_{P,\text{total}}$	–	Experiment A: 0.13 Experiment B: 0.58	fraction of total attached *E. coli*	Walters *et al.* (2013)
$f_{TSS,j}$	–	see Table 2	percentage of particle class *j*	Walters (2013)
h	m	0.5	water depth	Walters *et al.* (2014b)
I_0	Watt m^{-2}	Experiment A: 6.5 Experiment B: 17	average surface UV irradiance	Walters *et al.* (2014b)
I_e	Watt m^{-2}	$I_e=\frac{I_0}{k_{att}h}(1-e^{-k_{att}h})$	average UV irradiance in the epilimnion	Auer & Niemaus (1993)
m_α	–	53	parameter of α	calibrated
m_k	–	0.16	parameter of k_d	calibrated
n_α	–	−112	parameter of α	calibrated
n_k	–	−82	parameter of k_d	calibrated
ρ_j	kg m^{-3}	see Table 2	density of particle class *j*	calibrated
P	MPN $mgTSS^{-1}$	6,200	amount of *E. coli* associated with suspended particles	estimated
v_j	m h^{-1}	see Table 2	settling velocity of particle class *j*	Wu & Wang (2006)

Table 2 | Particle distribution in three cases and *E. coli* fraction to each particle size class

	Case 1	Case 2		Case 3		
	Class i	Class i	Class ii	Class i	Class ii	Class iii
Particle characteristics						
Median diameter (μm)	23	8	100	8	40	500
Density (kg m^{-3})	1,170	1,450	1,020	1,450	1,100	1,003
Settling velocity (m h^{-1})	0.13	0.04	0.28	0.04	0.22	1.01
Particle distribution in flume water $f_{TSS,j}$						
Experiment A (–)	1	0.17	0.83	0.14	0.60	0.26
Experiment B (–)	1	0.42	0.58	0.42	0.48	0.10
E. coli fraction associated with each particle size class $f_{P,j}$						
Experiment A & B (–)	1	0.04	0.96	0.04	0.88	0.08

The model included a TSS module and an *E. coli* module. In both modules, the influence of different particle size classes was investigated. For Experiment A the simulation started when the wastewater was added to the flume ($t = 0$). Since Experiment B was performed as a resuspension experiment, the simulation began after resuspension was induced by increasing the volumetric flow rate to 0.2 m^3 s^{-1}. Namely Experiment B simulated how the resuspended particles settled down and how *E. coli* were removed from the water column after resuspension. In the *E. coli* module, neither resuspension nor a transient effect from the bottom sediment zone (Ghimire & Deng 2013; Yakirevich *et al.* 2013) were considered, because *E. coli* concentrations in the bed sediment before and after adding the wastewater were low (Walters *et al.* 2014b).

TSS module

The TSS module describes dispersion and settling processes. Three separate cases have been simulated by incorporating either one, two, or three particle size classes referred to as Case 1, Case 2, and Case 3, respectively. The TSS concentration has been simulated using the following equations:

$$C_{TSS} = \sum_{j=1}^{n} C_{TSS,j} \tag{1}$$

$$\frac{\partial C_{TSS,j}}{\partial t} = D\frac{\partial^2 C_{TSS,j}}{\partial x^2} - v_j\frac{\partial C_{TSS,j}}{\partial x} \tag{2}$$

where n is the number of particle size classes, C_{TSS} is the overall TSS concentration, $C_{TSS,j}$ is the TSS concentration of particle size class j, and v_j is the settling velocity of particle size class j. The calculation of settling velocity v_j involves the particle density and particle size (Wu & Wang 2006), D is the dispersion coefficient and x represents the vertical axis. The initial condition of $C_{TSS,j}$ is described by Equation (3). $f_{TSS,j}$ is the percentage of particle class j at $t = 0$ (Table 2). Equations (4) and (5) represent the lower ($x_{0.5}$) and upper (x_0) boundary condition.

$$C^0_{TSS,j} = f_{TSS,j}\, C^0_{TSS} \tag{3}$$

$$D\frac{\partial C_{TSS,j}}{\partial x}(x_{0.5}) = 0 \tag{4}$$

$$D\frac{\partial C_{TSS,j}}{\partial x}(x_0) = 0 \tag{5}$$

E. coli module

The total *E. coli* concentration was partitioned into freely suspended and particle-associated *E. coli*. The particle-associated bacteria were further fractionated into different particle size classes as described in the TSS module for Case 2 and Case 3.

$$C_{EC} = C_F + C_P \tag{6}$$

$$C_P = \sum_{j=1}^{n} C_{P,j} \tag{7}$$

where C_{EC} is total *E. coli* concentration, C_F and C_P are the concentrations of freely suspended and particle-associated bacteria. $C_{P,j}$ represents the concentration of *E. coli* attached to particle size class *j*.

E. coli has a mass density slightly higher than water (Godin *et al.* 2007). Thus, the settling velocity of freely suspended *E. coli* was calculated to be more than 50 times lower compared to that of the smallest particle class. Therefore the settling mechanism of freely suspended *E. coli* was neglected and the particle-associated bacteria were assumed to have the same settling velocity as the particles they were associated with. *E. coli* fate and transport equations are presented in Equations (8) and (9).

$$\frac{\partial C_F}{\partial t} = D\frac{\partial^2 C_F}{\partial x^2} - F_{sun}\, k_{UV}\, C_F - k_d\, C_F \qquad (8)$$

$$\frac{\partial C_{P,j}}{\partial t} = D\frac{\partial^2 C_{P,j}}{\partial x^2} - v_j\frac{\partial C_{P,j}}{\partial x} - F_{sun} k_{UV}\, C_{P,j} - k_d\, C_{P,j} \qquad (9)$$

where

$$k_{att} = 0.13\, C_{TSS} + 0.27 \qquad (10)$$

$$I_e = \frac{I_0}{k_{att} h}\left(1 - e^{-k_{att} h}\right) \qquad (11)$$

$$k_{UV} = 3600\ \alpha\, I_e \qquad (12)$$

$$\alpha = m_\alpha\, e^{n_\alpha C_{TSS}} \qquad (13)$$

$$k_d = m_k\, e^{n_k C_{TSS}} \qquad (14)$$

Note that k_d is the natural inactivation coefficient and k_{UV} is the UV inactivation coefficient. F_{sun} is a Boolean variable being '1' during daytime and '0' during nighttime and activates or deactivates the UV inactivation mechanism. k_{att} is the average vertical attenuation coefficient. The equation for k_{att} was determined by additional laboratory experiments using heavily TSS-laden water from the flume system (Walters 2013). I_e is the depth-average UV irradiance in the water column and was calculated according to Auer & Niemaus (1993). I_0 is the average surface UV irradiance at daytime and h is the water depth (0.5 m). The UV sensitivity coefficient α and natural inactivation coefficient k_d are assumed to be functions of the TSS concentration; m_α, n_α, m_k, and n_k are the parameters of the functions used to correlate α and k_d to the TSS concentrations. It is assumed that when the TSS concentration increases, α and k_d tend to be zero. Although the decay rates of suspended and particle-associated bacteria may differ, we assumed only one α and one k_d, avoiding a non-essential complexity of the model.

Jamieson *et al.* (2005) suggest that in a low ionic strength environment such as a freshwater stream, bacteria adsorption would be dominated by strong bonding mechanisms or irreversible attachment. Since the Obernach is an oligotrophic river, adsorption of *E. coli* to sediment particles was assumed to be irreversible. Initial conditions of the *E. coli* module are listed in Equations (15)–(17).

$$C_P^0 = C_{TSS}\, P = f_{P,\text{total}}\, C_{EC}^0 \qquad (15)$$

$$C_F^0 = (1 - f_{P,\text{total}})C_{EC}^0 \qquad (16)$$

$$C_{P,j}^0 = f_{P,j} C_P^0 \qquad (17)$$

Note that C_{EC}^0, C_P^0, C_F^0 and $C_{P,j}^0$ are the initial concentrations of total *E. coli*, attached *E. coli*, freely suspended *E. coli* and the *E. coli* attached to particle size class *j*. $f_{P,\text{total}}$ is the fraction of attached bacteria to total *E. coli* concentration at $t = 0$. $f_{P,j}$ represents the fraction of attached *E. coli* which are associated with particle size class *j* at $t = 0$. *P* is the amount of *E. coli* associated with suspended particles. George *et al.* (2004) found an approximately linear relationship between the percentage of *E. coli* associated with suspended particles and the TSS concentration. In this study, *P* was estimated to equal 6,200 MPN mgTSS^{-1}. The resulting fractions of attached bacteria $f_{P,\text{total}}$ are 13% in Experiment A and 58% in Experiment B, respectively. Those values are comparable to the values reported in literature. For example, Characklis *et al.* (2005) found an average of 20–35% of bacteria associated with particles in background samples and 30–55% in storm water samples. All parameters used within the simulations are summarized in Table 1. The boundary conditions of the *E. coli* module are similar to the TSS module.

RESULTS

Model calibration

With the data obtained from the field experiments as described in Walters *et al.* (2014b) and Walters (2013) a calibration procedure was used to determine the following unknown parameters: particle density of each particle size class ρ_j, UV sensitivity coefficient α, and the natural inactivation coefficient k_d. Simulated concentrations resemble the concentration at water depth of 0.25 m. Particle density and particle sizes were used to calculate the settling velocities. Estimation of the UV sensitivity coefficient α and the natural inactivation coefficient k_d was performed according to Equations (13) and (14), respectively. Firstly, the particle density of each particle size class was varied so that the simulated TSS concentrations closely agreed with the measured TSS concentrations over the experimental duration. Secondly, the optimized particle densities were incorporated into the settling mechanism of the *E. coli* module, and the four parameters m_α, n_α, m_k, and n_k were varied so that the model output closely agreed with the measured *E. coli* concentrations. Calibrated particle densities are summarized in Table 2. The expressions of α and k_d are as follows: $\alpha = 53\, e^{-112\, C_{TSS}}$ and $k_d = 0.16\, e^{-82\, C_{TSS}}$.

Effect of particle size distribution on the simulation of TSS and *E. coli* concentrations

Table 2 presents the different particle size classes and properties used to investigate the influence of particle size classes on the model performance. The calibrated densities in Case 2 are as follows: $\rho_1 = 1{,}450$ kg m^{-3} ($d_1 = 8$ μm) and $\rho_2 = 1{,}020$ kg m^{-3} ($d_2 = 100$ μm). In most mineral soils, the dry density varies from 1,100 to 1,600 kg m^{-3} (Hillel 1980). Therefore the calibrated density values can be assumed to be acceptable.

The observed and predicted TSS as well as *E. coli* concentrations for the three cases are shown in Figures 1 and 2, respectively. In Figure 1(a) and 1(d) it can be seen that the model does not fit the measured TSS concentrations optimally when only one particle size class was incorporated in the model ($d_1 = 23$ μm, see Table 2). For Case 2 (Figure 1(b) and 1(e)) and Case 3 (Figure 1(c) and 1(f)), where more than one particle size class was defined, predictions of the TSS concentrations were obviously enhanced. The normalized root-mean-square deviation (NRMSD) improved from 15.2% (Figure 1(a)) to 10.3% (Figure 1(c)) in Experiment A and from 9.3% (Figure 1(d)) to 4.0% (Figure 1(f)) in Experiment B when three particle size classes were incorporated.

Figure 2 presents the simulation results of *E. coli* for the three cases. Here it can be seen that the particle size distribution has a similar impact on the simulated *E. coli*

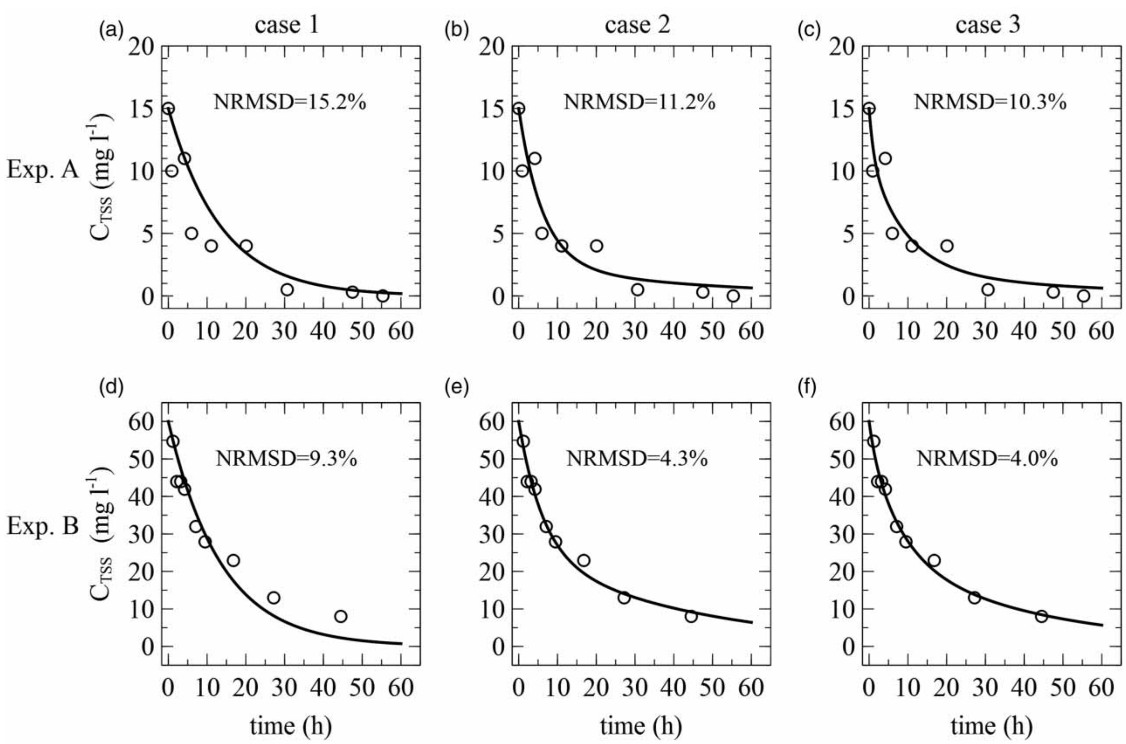

Figure 1 | Influence of the particle size distribution on the simulated TSS concentrations in Experiments A (top row) and B (bottom row). Simulation results depend on either one (a), (d), two (b), (e), or three (c), (f) particle size classes. Measured values are average values of three samples and indicated by circles. NRMSD is normalized root-mean-square deviation quantifying the difference between the measured values and the simulation results.

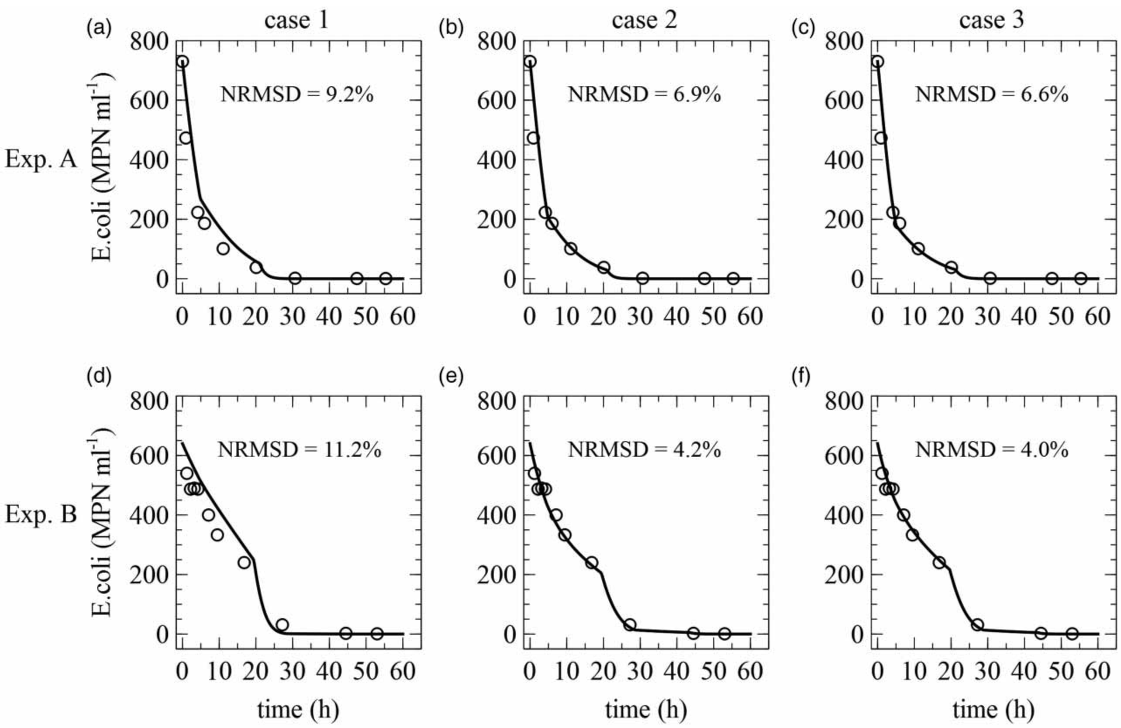

Figure 2 | Influence of the particle size distribution on the simulation of *E. coli* concentrations in Experiments A (top row) and B (bottom row). Simulation results depend on either one (a), (d), two (b), (e), or three (c), (f) particle size classes. Measured values are average values of three samples and indicated by circles. NRMSD is normalized root-mean-square deviation.

and TSS concentrations. The simulation results for *E. coli* in Cases 2 and 3 fit the experimental data much better than Case 1. Based on the NRMSD, the accuracy of the model using three particle size classes (Case 3) is only slightly improved (less than 1% NRMSD difference) compared to two classes (Case 2) in both experiments. Therefore, all further simulations were performed with only two particle size classes.

Model improvement by integration of TSS concentration-dependent parameters

Usually α and k_d are constants in a model (Jamieson *et al.* 2005; Cho *et al.* 2010). This study compared the performance of the model incorporating constant (Figure 3(a) and 3(b)) and TSS concentration-dependent values for α and k_d (Figure 3(c) and 3(d)). Figure 3(a) and 3(b) show that the calibrated values of α ($18\,m^2\,MJ_{UV}^{-1}$) and k_d ($0.09\,h^{-1}$) in Experiment A are seven to nine times higher than α ($2\,m^2\,MJ_{UV}^{-1}$) and k_d ($0.01\,h^{-1}$) in Experiment B. This indicates a higher *E. coli* removal rate in Experiment A although the average UV irradiance in Experiment B was twice as high as in Experiment A (see Table 1). It is hypothesized that the sudden increase in flow rate in Experiment B led to the resuspension of fine bed sediments in the water column, which delayed the *E. coli* removal. A similar hypothesis was proposed by de Brauwere *et al.* (2011) who found their model underestimating the *E. coli* concentrations in the maximum turbidity zone of an estuary. They suggested that this occurred because the *E. coli* dynamics were modelled independent of the suspended matter.

In order to correlate the *E. coli* removal rate with the TSS concentration, α and k_d were assumed to be exponential functions of the TSS concentration in this study. The calibrated results were $\alpha = 53\,e^{-112\,C_{TSS}}$ and $k_d = 0.16\,e^{-82\,C_{TSS}}$ as previously mentioned. Generally, the uniform expressions for α and k_d gave a good prediction in both experiments, and simulations with TSS-dependent parameters showed better consonance with the observed values. A more obvious model improvement can be seen in Figure 3(b) and 3(d) for Experiment B compared to Experiment A (see Figure 3(a) and 3(c)). A possible explanation for this trend is that Experiment A had an initial TSS concentration of $C_{TSS}^0 = 15\,mg\,l^{-1}$. The variation of the TSS concentration had less influence on α and k_d compared to Experiment B where the initial TSS concentration was four times higher ($C_{TSS}^0 = 60\,mg\,l^{-1}$). Therefore, it is

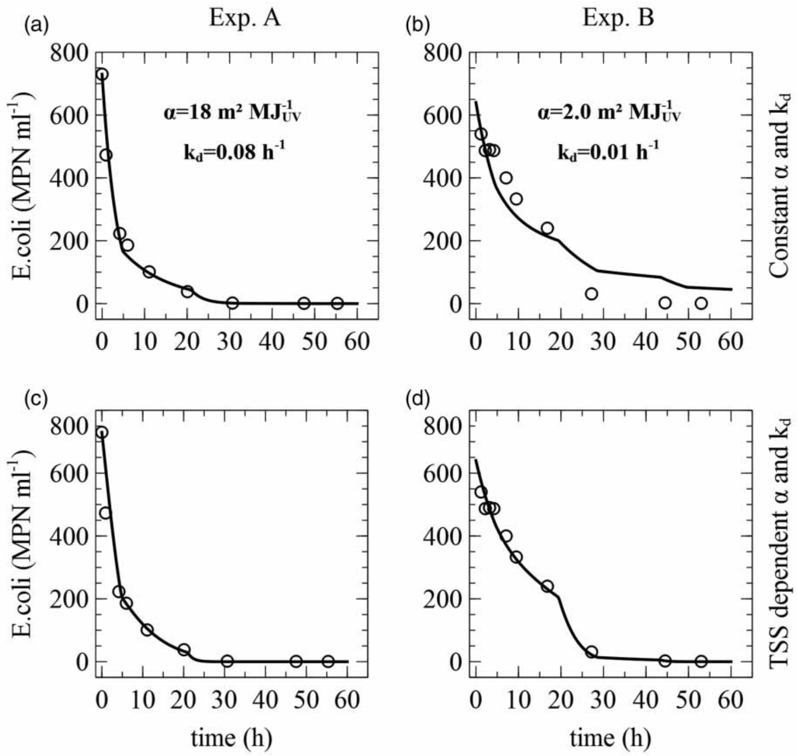

Figure 3 | Comparison of models incorporating constant parameters and TSS-dependent parameters in both experiments. The top row shows simulation with constant parameters and the bottom with TSS-dependent parameters. Measured values are average values of three samples and indicated by circles.

possible to use constant α and k_d in the *E. coli* removal model when the TSS concentration is low or constant. Otherwise, a TSS-dependent parameter will more accurately simulate the UV and natural inactivation processes.

Influence of each mechanism on the removal of *E. coli*

Figure 4 shows the influence of each individual mechanism in Experiments A (Figure 4(a)–4(d)) and B (Figure 4(e)–4(h)),

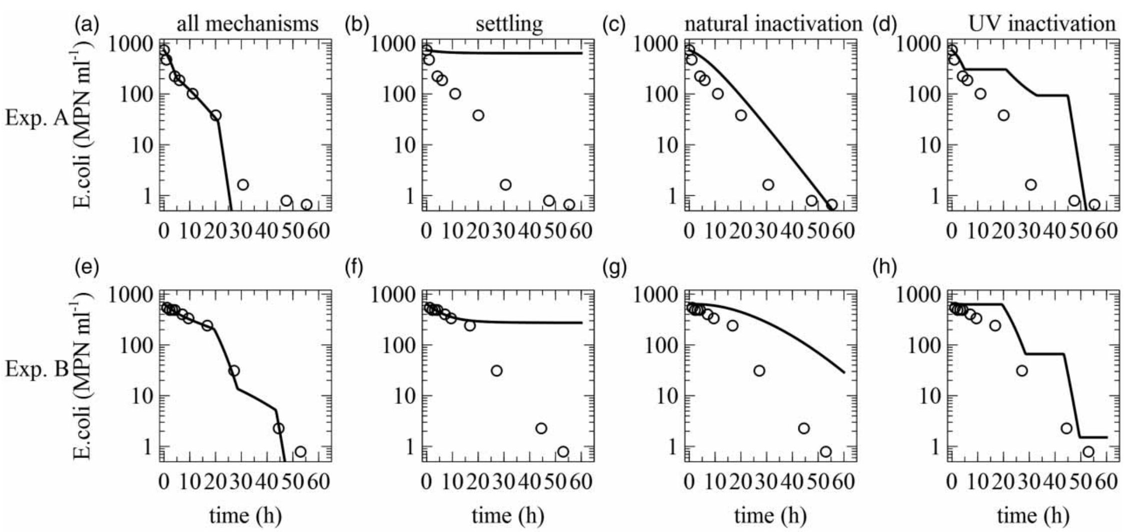

Figure 4 | Impact of the three different removal mechanisms on the prediction of *E. coli* concentrations in the water column throughout Experiment A (top row) and Experiment B (bottom row). Plots (a) and (e) show the simulation with all three mechanisms, plots (b) and (f) show the impact of the particle settling, plots (c) and (g) show the impact of die-off, plots (d) and (h) show the impact of UV inactivation. Measured values are average values of three samples and indicated by circles.

respectively. Note that Figure 4(a) and 4(e) illustrate the same measured and predicted values as in Figure 3(c) and 3(d), but subfigures in Figure 4 are logarithmically scaled. When settling was the only mechanism considered, UV and natural inactivation coefficients were assumed to equal zero. When only natural or UV inactivation was simulated, the suspended particles were assumed to deposit and *E. coli* were assumed to be completely freely suspended without being influenced by sedimentation.

Figure 4(b) and 4(f) show that the settling mechanism removed bacteria from the water column only at the beginning of the experiments. This is because a large portion of particles settled out of the water column within the first 20 hours (Figure 1). Moreover, the settling mechanism had almost no effect in Experiment A (Figure 4(b)) due to the low TSS concentration and *E. coli* attachment rate. The natural inactivation rate was low at the beginning in Experiment B, due to a higher TSS concentration of 60 mg l^{-1}, and increased gradually (Figure 4(g)). In contrast, the natural inactivation rate in Experiment A was relatively high, because of a four times lower initial TSS concentration of 15 mg l^{-1} (Figure 4(c)). Solar inactivation only occurs during the daytime, explaining the stepwise reduction seen in Figure 4(d) and 4(h).

Sensitivity analysis of the *E. coli* concentration prediction

Table 3 shows the ranking of the absolute–relative sensitivity analysis for *E. coli* modelling in both experiments using AQUASIM. Density of particle class II (ρ_2) and initial TSS concentration C^0_{TSS} were the most sensitive parameters in both experiments. Densities of the particles were used to calculate the settling velocity of the particles as well as of *E. coli*. Initial TSS concentrations are essential in this model since the TSS concentration at a later simulation time depends on it. Furthermore, the vertical attenuation coefficient k_{att}, the UV sensitivity coefficient α, and the natural inactivation coefficient k_d are all related to the TSS concentration.

The total percentage of attached *E. coli*, $f_{P,\text{total}}$, was more sensitive in Experiment B (ranked 2nd) compared to Experiment A (ranked 12th). In this study, 58% of *E. coli* in Experiment B were particle-associated compared to 13% in Experiment A. When more bacteria were attached to particles, the total bacterial concentration decreased more rapidly from the water column due to the settling mechanism. This is the reason for higher sensitivity of $f_{P,\text{total}}$ in Experiment B. The density of particle class I (ρ_1) ranked 10th and 4th in Experiments A and B, respectively.

Table 3 | Sensitivity analysis results for *E. coli* simulation

Ranking	Experiment A	Experiment B
1	ρ_2	ρ_2
2	C^0_{TSS}	$f_{P,\text{total}}$
3	$f_{TSS,2}$	C^0_{TSS}
4	n_α	ρ_1
5	I_0	$f_{TSS,1}$
6	m_α	n_k
7	m_k	$f_{P,2}$
8	n_k	n_α
9	$f_{TSS,1}$	m_k
10	ρ_1	$f_{TSS,2}$
11	$f_{P,2}$	$f_{P,\text{total}}$
12	$f_{P,\text{ total}}$	m_α
13	$f_{P,1}$	$f_{P,1}$
14	D	D

Since both $f_{P,\text{total}}$ and ρ_1 were more sensitive in Experiment B, it can be concluded that the settling process plays a more important role at elevated TSS concentrations.

On the other hand, the UV intensity I_0 and the UV sensitivity parameter m_α had a stronger influence on Experiment A (ranked 5th and 6th) compared to Experiment B (ranked 11th and 12th). This indicates that *E. coli* is more susceptible to UV intensity variations, when less particulate matter is present, such as in Experiment A.

The impacts of three main parameters, C^0_{TSS}, m_α, and $f_{P,\text{total}}$, on the *E. coli* removal process have been assessed. Figure 5 illustrates the simulation results when these parameters were changed by 50% or 200% of the original parameter value. From Figure 5 it can clearly be seen that (i) C^0_{TSS} was sensitive in both experiments, (ii) m_α was more sensitive in Experiment A where there was less TSS, and (iii) $f_{P,\text{total}}$ was more influential in Experiment B.

DISCUSSION

Impact of two particle size classes on the accuracy of the model

There have been many attempts to investigate the influence of the settling velocity distribution on the sedimentation process in retention tanks and to incorporate more than one particle size class into particle (TSS) settling models (Huebner & Geiger 1996; Maruejouls *et al.* 2012). However, there is still no

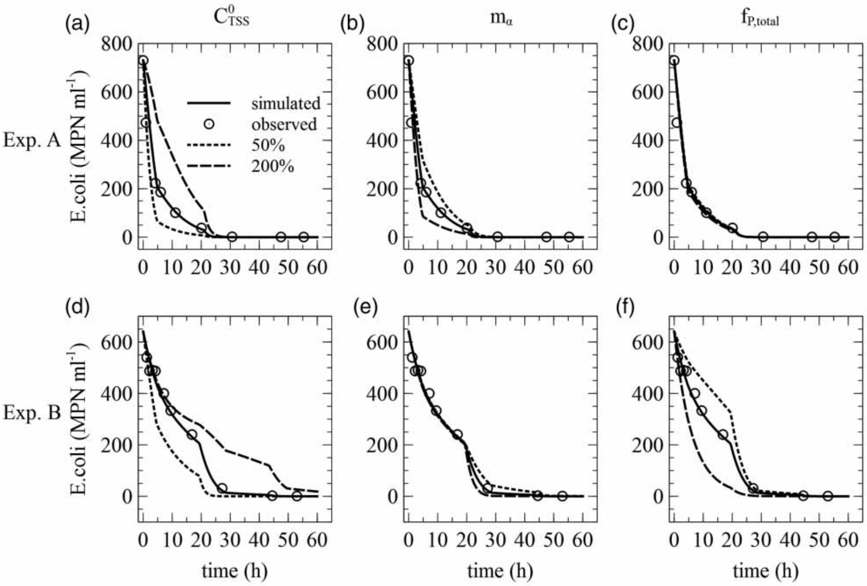

Figure 5 | Assessment of the impacts of the major parameters C^0_{TSS}, m_α and $f_{P,\mathrm{total}}$ on the *E. coli* removal process. Plots (a) to (c) refer to Experiment A and plots (d) to (f) refer to Experiment B. Measured values are average values of three samples and are indicated by circles.

application of it to the transport of FIB in aquatic water quality models. Some FIB transport models for flood events encounter overestimation of the FIB concentration directly after the hydraulic peak, followed by an underestimation (Jamieson *et al.* 2005; Gao *et al.* 2011; Ghimire & Deng 2013). This problem can be due to the incorporation of only one particle size class (constant settling velocity). In such cases, the settling velocity in the model may be lower than what actually occurs after the hydraulic peak where large particles and attached FIB are removed from the water column. Afterwards, the median settling velocity is overestimated as in reality the majority of particles remaining in the water column are small and settle slower.

In this study, the partitioning of particles into two particle size classes provided a more accurate and smooth removal prediction of *E. coli* compared to only one particle size class. According to section Influence of each mechanism on the removal of *E. coli*, the settling mechanism for *E. coli* removal is more influential when the TSS concentration increases. It can therefore be inferred that incorporating two particle size classes is definitely improving the prediction of FIB transport during CSOs when TSS concentrations are elevated (typically above 100 mg l^{-1}).

Incorporation of TSS concentration-dependent parameters

This study attempted to find flexible equations for α and k_d to fit FIB decay mechanisms at different TSS concentrations. α and k_d were 8.5 m² MJ_{UV}^{-1} and 0.047 h^{-1}, respectively, when the initial TSS concentration was 15 mg l^{-1}. Sinton *et al.* (2002) obtained solar sensitivity coefficients ranging from 0.277 to 0.395 m² MJ_{solar}^{-1} in fresh river water. Since they used solar intensity instead of UV intensity (3% of the total energy of sunlight is UV), their UV sensitivity coefficient would reach 9.1 to 13.1 m² MJ_{UV}^{-1}, which is comparable to our reported values. They further found the dark die-off coefficients for *E. coli* to vary from 0.001 to 0.043 h^{-1}, which aligns well with our study (0.047 h^{-1} when TSS = 15 mg l^{-1}), justifying the derived expressions for α and k_d.

In this study it was assumed that as the TSS concentration increased, *E. coli* persistence in the water column would be augmented. The prolonged survival of enteric bacteria in river bed sediments compared to that in the water column has long been recognized (Sherer *et al.* 1992; Davies *et al.* 1995; Craig *et al.* 2002; Pachepsky & Shelton 2011). Likewise, for similar reasons the presence of suspended solids has also been linked with growth and survival of *E. coli* in the water column. Desmarais *et al.* (2002) found that adding sterile sediment to river water causes the *E. coli* population in the water column to regrow proportional to the amount of sediment added. Additionally, suspended particulate matter is also known to reduce the transmission of solar irradiation and therefore lowers the solar inactivation of microorganisms by shading and encasement (Dickenson & Sansalone 2012; Kollu &

Ormeci 2012). Whitby & Palmateer (1993) discovered a linear relationship between the TSS concentration and the number of FC in the effluent of wastewater treatment plants after UV disinfection. Hence, the correlation of the TSS concentration to the removal rate of bacteria as performed in this study is a necessity to achieve a precise model prediction of the FIB transport.

E. coli removal mechanisms and patterns

Experiments A and B were dominated by different removal mechanisms (Figure 4). Figure 4(b)–4(d) show that natural and UV inactivation were the main removal mechanisms in Experiment A, because the sedimentation effect was very low throughout the whole experiment. Meanwhile, Figure 4(f)–4(h) indicate that the settling mechanism was the dominant removal mechanism during the first 20 hours in Experiment B, and afterwards natural and UV inactivation predominated.

Figure 4(a) and 4(e) additionally give insight into the different inactivation patterns of *E. coli* in Experiments A and B. Experiment A exhibited a fast removal for the first 30 hours and a tailing towards equilibrium at the end. Experiment B showed a lower removal during the first 20 hours followed by a fast removal. Blaustein *et al.* (2013) reported that most often the measured FIB decay patterns are of the type seen in Experiment A. The tailing in Experiment A is probably due to the fact that the carrying capacity of the environment is reached and the bacteria concentration remains at the background level (Easton *et al.* 2005; Blaustein *et al.* 2013). Furthermore, the inactivation patterns in wastewater are mostly the type observed in Experiment B (Blaustein *et al.* 2013), probably due to higher TSS concentrations and better nutrient supply. In this model, UV and natural inactivation rates were very high at the end of the experiment because of low TSS concentrations. In consequence the model did not perform well when the *E. coli* concentration began to level off and approached background concentrations less than 5 MPN ml^{-1} (see Figure 4(a) and 4(e)). Since the focus of this study was to investigate the transport of FIB after CSOs, the prediction of such low MPN concentrations was not the main interest.

CONCLUSIONS

The fate and transport of *E. coli* were investigated experimentally at large scale and subsequently described by a modelling approach. A 1D model was developed to predict the TSS and *E. coli* concentrations under steady flow conditions throughout the experimental duration of 70 hours. The conclusions of the study are as follows.

1. Incorporating only a single particle size class results in an insufficient prediction of the TSS and *E. coli* concentrations in the water column. The model performs well when at least two particle size classes are included. The accuracy of the model could only be slightly improved by incorporating a third particle size class.
2. *E. coli* dynamics were considered to be dependent on the TSS concentration. The UV sensitivity coefficient α and natural inactivation coefficient k_d were related to the TSS concentrations by an exponential expression. Thus, the model was capable of predicting *E. coli* concentrations accurately at different TSS levels. At high initial TSS concentrations ($\geq$ 60 mg l^{-1}), incorporation of TSS-dependent α and k_d resulted in an obvious improvement of the model performance. Constant α and k_d values were sufficient to predict UV and natural inactivation when the initial TSS concentration was low.
3. Depending on the size and concentration of particles in the water column, *E. coli* removal is dominated by different removal mechanisms. The results revealed that the sedimentation process was more important under higher TSS concentrations. In contrast, bacteria were more susceptible to solar irradiance and other natural inactivation processes, when less suspended particulate matter was present.

ACKNOWLEDGEMENTS

The authors gratefully acknowledge the research and infrastructure funding received from the German Research Foundation (DFG HO 1910/9-1 and RU 1546/2-1) and the Oswald-Schulze Foundation (OSS 1596/11).

REFERENCES

Alimova, A., Roberts, M., Katz, A., Rudolph, E., Steiner, J. C., Alfano, R. R. & Gottlieb, P. 2007 Effects of smectite clay on biofilm formation by microorganisms. *Biofilms* **3**, 47–54.

Auer, M. T. & Niemaus, S. L. 1993 Modeling fecal coliform bacteria – I. Field and laboratory determination of loss kinetics. *Water Res.* **27**, 693–701.

Blaustein, R. A., Pachepsky, Y., Hill, R. L., Shelton, D. R. & Whelan, G. 2013 *Escherichia coli* survival in waters: temperature dependence. *Water Res.* **47**, 569–578.

Canteras, J. C., Juanes, J. A., Pérez, L. & Koev, K. N. 1995 Modelling the coliforms inactivation rates in the Cantabrian Sea (Bay of Biscay) from in situ and laboratory determinations of t90. *Water Sci. Technol.* **32**, 37–44.

Characklis, G. W., Dilts, M. J., Simmons, O. D., Likirdopulos, C. A., Krometis, L.-A. H. & Sobsey, M. D. 2005 Microbial partitioning to settleable particles in stormwater. *Water Res.* **39**, 1773–1782.

Cho, K. H., Pachepsky, Y. A., Kim, J. H., Guber, A. K., Shelton, D. R. & Rowland, R. 2010 Release of *Escherichia coli* from the bottom sediment in a first-order creek: experiment and reach-specific modeling. *J. Hydrol.* **391**, 322–332.

Cho, K. H., Pachepsky, Y. A., Kim, J. H., Kim, J.-W. & Park, M.-H. 2012 The modified SWAT model for predicting fecal coliforms in the Wachusett Reservoir Watershed, USA. *Water Res.* **46**, 4750–4760.

Craig, D. L., Fallowfield, H. J. & Cromar, N. J. 2002 Comparison of decay rates of faecal indicator organisms in recreational coastal water and sediment. *Water Sci. Technol.* **2**, 131–138.

Davies, C. M. & Bavor, H. J. 2000 The fate of stormwater-associated bacteria in constructed wetland and water pollution control pond systems. *J. Appl. Microbiol.* **89**, 349–360.

Davies, C. M., Long, J. A., Donald, M. & Ashbolt, N. J. 1995 Survival of fecal microorganisms in marine and freshwater sediments. *Appl. Environ. Microbiol.* **61**, 1888–1896.

De Brauwere, A., de Brye, B., Servais, P., Passerat, J. & Deleersnijder, E. 2011 Modelling *Escherichia coli* concentrations in the tidal Scheldt river and estuary. *Water Res.* **45**, 2724–2738.

Decamp, O. & Warren, A. 2000 Investigation of *Escherichia coli* removal in various designs of subsurface flow wetlands used for wastewater treatment. *Ecol. Eng.* **14**, 293–299.

Desmarais, T. R., Solo-Gabriele, H. M. & Palmer, C. J. 2002 Influence of soil on fecal indicator organisms in a tidally influenced subtropical environment. *Appl. Environ. Microbiol.* **68**, 1165–1172.

Dickenson, J. A. & Sansalone, J. J. 2012 Distribution and disinfection of bacterial loadings associated with particulate matter fractions transported in urban wet weather flows. *Water Res.* **46**, 6704–6714.

Easton, J. H., Gauthier, J. J., Lalor, M. M. & Pitt, R. E. 2005 Die-off of pathogenic *E. coli* 157:H7 in sewage contaminated waters. *J. Am. Water Resour. Assoc.* **41**, 1187–1193.

EEA (European Environment Agency) 2015 *European Bathing Water Quality in 2014*. Report No. 1/2015. http://www.eea.europa.eu/publications/european-bathing-water-quality-in-2014 (accessed 20 May 2015).

Evison, L. M. 1989 Comparative study on the survival of indicator organisms and pathogens in fresh and sea water. *Water Sci. Technol.* **20**, 309–315.

Gao, G., Falconer, R. A. & Lin, B. 2011 Numerical modelling of sediment–bacteria interaction processes in surface waters. *Water Res.* **45**, 1951–1960.

Garzio-Hadzick, A., Shelton, D. R., Hill, R. L., Pachepsky, Y. A., Guber, A. K. & Rowland, R. 2010 Survival of manure-borne *E. coli* in streambed sediment: effects of temperature and sediment properties. *Water Res.* **44**, 2753–2762.

George, I., Anzil, A. & Servais, P. 2004 Quantification of fecal coliform inputs to aquatic systems through soil leaching. *Water Res.* **38**, 611–618.

Ghimire, B. & Deng, Z. 2013 Hydrograph-based approach to modeling bacterial fate and transport in rivers. *Water Res.* **47**, 1329–1343.

Godin, M., Bryan, A. K., Burg, T. P., Babcock, K. & Manalis, S. R. 2007 Measuring the mass, density, and size of particles and cells using a suspended microchannel resonator. *Appl. Phys. Lett.* **91**, 1–3.

Hillel, D. J. 1980 *Fundamentals of Soil Physics*. Academic Press, New York.

Howell, J. M., Coyne, M. S. & Cornelius, P. L. 1996 Effect of sediment particle size and temperature on fecal bacteria mortality rates and the fecal coliform/fecal streptococci ratio. *J. Environ. Qual.* **25**, 1216–1220.

Huebner, M. & Geiger, W. F. 1996 Characterisation of the performance of an off line storage tank. *Water Sci. Technol.* **34**, 25–32.

Jamieson, R., Joy, D. M., Lee, H., Kostaschuk, R. & Gordon, R. 2005 Transport and deposition of sediment-associated *Escherichia coli* in natural streams. *Water Res.* **39**, 2665–2675.

Jeng, H. C., England, A. J. & Bradford, H. B. 2005 Indicator organisms associated with stormwater suspended particles and estuarine sediment. *J. Environ. Sci. Health* **40**, 779–791.

Jobson, H. E. & Sayre, W. W. 1970 Vertical transfer in open channel flow. *J. Hydraul. Div.* **96**, 703–724.

Kay, D., Stapleton, C. M., Wyer, M. D., McDonald, A. T., Crowther, J., Paul, N., Jones, K., Francis, C., Watkins, J., Wilkinson, J., Humphrey, N., Lin, B., Yang, L., Falconer, R. A. & Gardner, S. 2005 Decay of intestinal enterococci concentrations in high-energy estuarine and coastal waters: towards real-time T90 values for modelling faecal indicators in recreational waters. *Water Res.* **39**, 655–667.

Kollu, K. & Ormeci, B. 2012 Effect of particles and bioflocculation on ultraviolet disinfection of *Escherichia coli*. *Water Res.* **46**, 750–760.

Maruejouls, T., Vanrolleghem, P. A., Pelletier, G. & Lessard, P. 2012 A phenomenological retention tank model using settling velocity distributions. *Water Res.* **46**, 6857–6867.

Nagels, J. W., Davies-Colley, R. J., Donnison, A. M. & Muirhead, R. W. 2002 Faecal contamination over flood events in a pastoral agricultural stream in New Zealand. *Water Sci. Technol.* **45**, 45–52.

Pachepsky, Y. A. & Shelton, D. R. 2011 *Escherichia coli* and fecal coliforms in freshwater and estuarine sediments. *Crit. Rev. Environ. Sci. Technol.* **41**, 1067–1110.

Pommepuy, M., Guillaud, J. F., Dupray, E., Derrien, A., Guyader, F. & Le Cormier, M. 1992 Enteric bacteria survival factors. *Water Sci. Technol.* **25**, 93–103.

Qualls, R. G., Ossoff, S. F., Chang, J. C. H., Dorfman, M. H., Dumais, M., Lobe, D. C., Johnson, J. D. & Quails, R. G. 1985 Factors controlling sensitivity in ultraviolet disinfection of secondary effluents. *J. Water Pollut. Control Fed.* **57**, 1006–1011.

Reichert, P. 1994 Aquasim–A tool for simulation and data analysis of aquatic systems. *Water Sci. Technol.* **30**, 21–30.

Schultz-Fademrecht, C., Wichern, M. & Horn, H. 2008 The impact of sunlight on inactivation of indicator microorganisms both in river water and benthic biofilms. *Water Res.* **42**, 4771–4779.

Sherer, B. M., Miner, J. R., Moore, J. A. & Buckhouse, J. C. 1992 Indicator bacterial survival in stream sediments. *J. Environ. Qual.* **21**, 591–595.

Sinton, L. W., Hall, C. H., Lynch, P. A. & Davies-colley, R. J. 2002 Sunlight inactivation of fecal indicator bacteria and bacteriophages from waste stabilization pond effluent in fresh and saline waters. *Appl. Environ. Microbiol.* **68**, 1122–1131.

Steets, B. M. & Holden, P. A. 2003 A mechanistic model of runoff-associated fecal coliform fate and transport through a coastal lagoon. *Water Res.* **37**, 589–608.

Walters, E. M. 2013 Fate and transport of fecal indicator bacteria in flume systems mimicking an oligotrophic river. PhD thesis. https://mediatum.ub.tum.de/doc/1174099/1174099.pdf.

Walters, E., Graml, M., Behle, C., Müller, E. & Horn, H. 2013 Influence of particle association and suspended solids on UV inactivation of fecal indicator bacteria in an urban river. *Water Air Soil Pollut.* **225**, 1822.

Walters, E., Kätzl, K., Schwarzwälder, K., Rutschmann, P., Müller, E. & Horn, H. 2014a Persistence of fecal indicator bacteria in sediment of an oligotrophic river: comparing large and lab-scale flume systems. *Water Res.* **61**, 276–287.

Walters, E., Schwarzwälder, K., Rutschmann, P., Müller, E. & Horn, H. 2014b Influence of resuspension on the fate of fecal indicator bacteria in large-scale flumes mimicking an oligotrophic river. *Water Res.* **48**, 466–477.

Whitby, G. E. & Palmateer, G. 1993 The effect of UV transmission, suspended solids and photoreactivation on microorganisms in wastewater treated with UV light. *Water Sci. Technol.* **27**, 379–386.

Wright, D. A., Killham, K., Glover, L. A. & Prosser, J. I. 1995 Role of pore size location in determining bacterial activity during predation by protozoa in soil. *Appl. Environ. Microbiol.* **61**, 3537–3543.

Wu, W. & Wang, S. S. Y. 2006 Formulas for sediment porosity and settling velocity. *J. Hydraul. Eng.* **132**, 858–862.

Yakirevich, A., Pachepsky, Y. A., Guber, A. K., Gish, T. J., Shelton, D. R. & Cho, K. H. 2013 Modeling transport of *Escherichia coli* in a creek during and after artificial high-flow events: three-year study and analysis. *Water Res.* **47**, 2676–2688.

First received 1 April 2015; accepted in revised form 13 November 2015. Available online 7 December 2015